

Heterotopic osteogenesis induced by implantation of allogenic bone matrix graft into mouse muscle perimysium. A morphometric study

Osteogênese heterotópica induzida pela implantação de enxerto de matriz óssea alogênica no perimílio de músculo de camundongo. Estudo morfométrico

Renato Faria Yassutaka YAEDÚ*

Fernanda Lourenço BRIGHENTTI*

Department of Biological Sciences, Laboratory of Histology – Dental School of Bauru – USP – São Paulo – Brazil

Tania Mary CESTARI

Graduate in Biological Sciences – Department of Biological Sciences, Laboratory of Histology - Dental School of Bauru – USP – São Paulo – Brazil

José Mauro GRANJEIRO DDS, PhD

Associate Professor – Department of Biological Sciences, Laboratory of Histology - Dental School of Bauru – USP – São Paulo – Brazil

Rumio TAGA DDS, PhD

Professor – Department of Biological Sciences, Laboratory of Histology - Dental School of Bauru – USP – São Paulo – Brazil

ABSTRACT

Heterotopic osteogenesis induced by allogenic bone matrix graft in the mouse muscle was analyzed by radiography, morphology and morphometry. Diaphyses of the femurs of 18 fifty-day-old mice were demineralized with 0.6 M HCl and implanted into the adductor muscle of the right thigh of 36 mice. Two, 5, 7, 14, 21 and 28 days after implantation, groups of 6 animals/period were sacrificed and radiographed, and specimens were collected and processed histologically. The presence of mineralized material in the graft was detected by radiography only on day 21. Morphologic and morphometric analysis of the histological sections showed that: a) the matrix remained intact up to day 7, followed by resorption of 16% by fibroblast-like mononuclear cells up to day 28; b) cartilage tissue was first detected on day 14 at the highest quantity observed in the experiment, occupying 5% of the graft volume and containing 4×10^2 chondrocytes/mm³ graft, followed by a substantial decline up to day 28 when it reached a volume density of 0.5% and 0.6×10^2 chondrocytes/mm³; c) bone cells and matrix were detected in minute amounts from day 14 on, with a volume density of 0.4% and containing 0.2×10^2 cells/mm³, which increased about 15 and 32 times, respectively, by the end of the 28-day, reaching 6% of the graft volume and 6×10^2 cells/mm³. We conclude that, despite the relatively low percentage of graft matrix resorption (total of 16%), the matrix was able to induce all events of the endochondral ossification cascade, i.e., formation and subsequent disappearance of hyaline cartilage, osteoblast differentiation, new bone formation and, later, the formation of hematogenous bone marrow.

UNITERMS

Bone transplantation; transplantation, homologous; ectopic, Osteogenesis, bone, morphometry, analisys; mouse

INTRODUCTION

One viable alternative for the treatment of extensive craniobuccofacial bone defects or of defects that are difficult to repair is the use of demineralized allogenic bone matrix graft submitted to special procedures for the elimination of potential ma-

trix antigen radicals^{10,25,26}. This therapeutic alternative has been proposed based on the pioneering discovery that organic bone matrix contains numerous soluble protein factors able to induce heterotopic osteogenesis by the mechanism of endochondral ossification^{17,19,23}. The matrix proteins, called bone morphogenetic proteins or BMPs, have been

isolated and purified from bone of various animals^{2,9,20,24,34}, and human BMPs have been produced and characterized by genetic recombination^{31,33,37}.

Despite the enormous scientific advances in the area of bone biology which have opened new perspectives for the treatment of perennital bone lesions, lyophilized human bone matrix continues to be widely used, especially in the field of dentistry. Thus, it is important to broaden the basic understanding of osteogenesis induced by allogenic bone matrix.

In the present morphometric study, we analyzed heterotopic osteogenesis induced by allogenic demineralized bone matrix implanted into the perimysium of the thigh muscle of mice by quantifying the disappearance of graft matrix, accumulation of cartilage, bone matrix and myeloid tissue, and growth of cartilage and bone cell populations. Radiographic control and qualitative histological analysis were also performed.

MATERIAL AND METHODS

Fifty-four fifty-day-old male Swiss mice weighing about 40g, obtained from the Central Animal House of the Bauru Dental School, were studied, with the animals receiving pelleted Purina ration and water *ad libitum* throughout the experiment.

Eighteen animals were sacrificed in order to obtain the femurs used for the preparation of the

block allogenic grafts of demineralized bone matrix. The remaining 36 animals were submitted to surgery for the implantation of the graft into the adductor muscle of the right thigh.

Preparation of the demineralized bone matrix graft

The epiphysis was removed from the collected femurs and the material was rigorously cleaned and stored under refrigeration at -18°C. The femurs were then demineralized in 0.6 M HCl under monitoring every 2 h by radiography, neutralized in 0.9% saline, cut into uniform 6mm long segments, and stored in 70% ethanol for a maximum period of three days²⁶.

Surgical procedures of graft implantation

Under general anesthesia with intraperitoneal injection of ketamine/xylazine (Agribrands do Brasil Ltda), all experimental animals were submitted to trichotomy of the right thigh, with a 1-cm incision being made in the tegumentum of the region with a N°. 11 surgical knife (Figure 1A) after vigorous disinfection with iodophor alcohol. The perimysium that separates the two bundles of the thigh adductor muscle was then pulled apart with scissors (Figure 1B), thus forming a pocket that received the graft (Figure 1C). The muscle fasciae were closed with resorbive No. 5-0 polyvicryl sutures and the tegumentum with No. 4-0 silk sutures (both Ethicon, Johnson & Johnson) (Figure 1D).

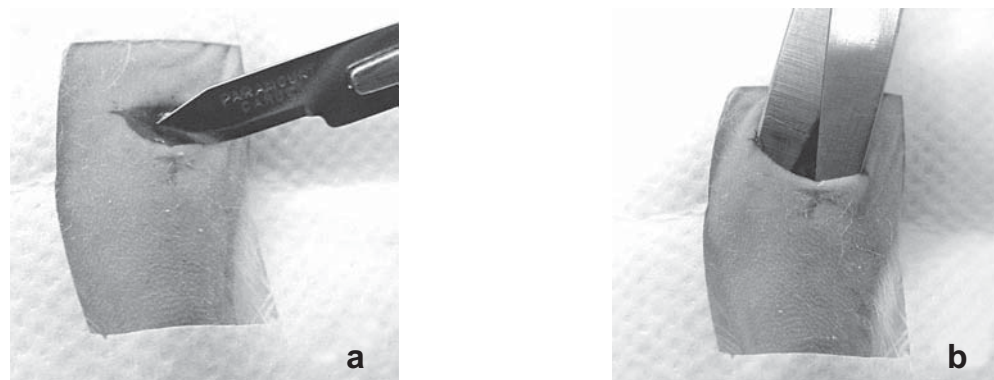


FIGURE 1 - Surgical procedures: **a**) 1-cm incision in the tegumentum; **b**) divulsion of the connective tissue between muscle fascias; **c**) graft implantation; and **d**) suture of the tegumentum.

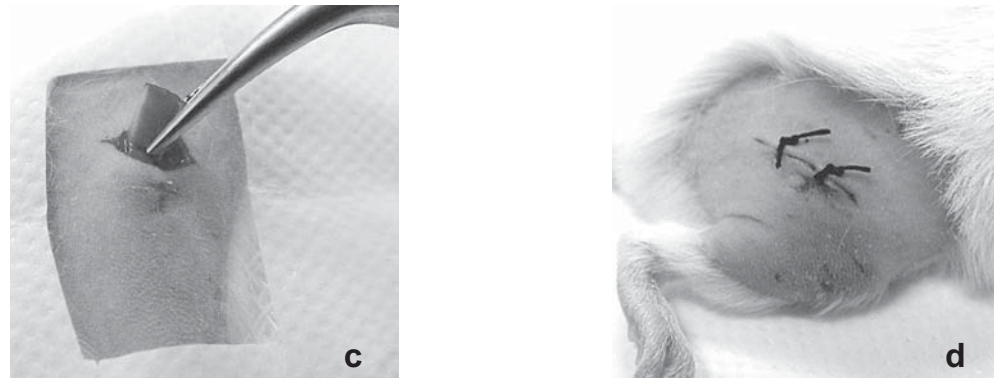


FIGURE 1 - Surgical procedures: **a**) 1-cm incision in the tegumentum; **b**) divulsion of the connective tissue between muscle fascias; **c**) graft implantation; and **d**) suture of the tegumentum.

General histological procedures

Mice of the experimental group were sacrificed by injection of an overdose of the anesthetic 2, 5, 7, 14, 21 and 28 days after graft implantation (six animals/period). After radiography, the implanted graft of each animal with surrounding reactional tissue was collected and fixed in 10% phosphate-buffered formalin for one week. The specimens were then demineralized in Morse solution (50% formic acid and 20% sodium citrate, 1:1), dehydrated in ethanol, cleared in xylene, and embedded in Histosec (paraffin + synthetic resin, Merck). The specimens were cut into 5 μ m thick alternating sections at 100 μ m intervals and stained with hematoxylin-eosin.

Morphometric analysis

A) Determination of volume density

Volume density, defined as the volume fraction of the entire graft occupied by a given component (demineralized matrix, resorption area, cartilage tissue, bone tissue and myeloid tissue), was determined with a digitalized Zeiss image analysis system consisting of an Axioskop 2 microscope, a Sony CCD-IRIS-RGB camera, Kontron K-300 software and an IBM microcomputer. Images from 25 histological fields selected by systematic randomization were captured on the microcomputer. In these images, the area of the graft occupied by each structure (A_i) and the total area examined (A) were

determined, and the volume density (V_{Vi}) of each type of structure was calculated according to the relation $V_{Vi} = AA_i = A_i/A$ (WEIBEL³², 1969).

B) Determination of the number of cartilage and bone cells in the graft

The number of cells per mm³ graft was determined by counting under a light microscope using a Zeiss integration II grid placed in a Zeiss Kpl 8X eyepiece and a Zeiss 100X oil immersion objective. The number of images of nuclei (n) of each cell type and the number of intersections (c) between these nucleus images and the ten parallel lines of the grid were counted in histological fields per fifty animals selected by systematic randomization. The number of cells (N) of each cell type was calculated according to the following formula:

$$N = \frac{2n \cdot V_p}{A (C/n \times d + 2t)}$$

(Aherne and Dunnill¹), where A = total area examined, d = distance between grid lines, t = section thickness, and V_p = processed volume.

Statistical analysis

All morphometric results were compared between groups by analysis of variance (ANOVA) and

means were contrasted by the Student-Newman-Keuls test using the Sigma Stat for Windows software (Jandel Scientific), with the level of significance set at 1 and 5%. Volume density values were submitted to statistical analysis after arc-sin transformation of the original data.

RESULTS

Radiographic results

Analysis of the radiographs obtained from the thigh region of animals submitted to allogenic graft implantation did not show any radiodense image indicative of new bone formation at 2, 5, 7 or 14 days post-implantation (see image of the last peri-

od in Figure 2a). In contrast, at 21 days, a thin radiodense line parallel to the femur was observed (Figure. 2b), indicating the presence of mineralized material. After 28 days, this radiodense line became thicker, demonstrating increased formation of mineralized material (Figure. 2c).

Morphologic results

At two days post-implantation, the old bone nutrient canals and lacunae of the osteocytes present in the graft were empty and the space of the medullary canal was filled with blood clots. Blood clots and an acute inflammatory infiltrate rich in polymorphonuclear neutrophils were observed outside the matrix.

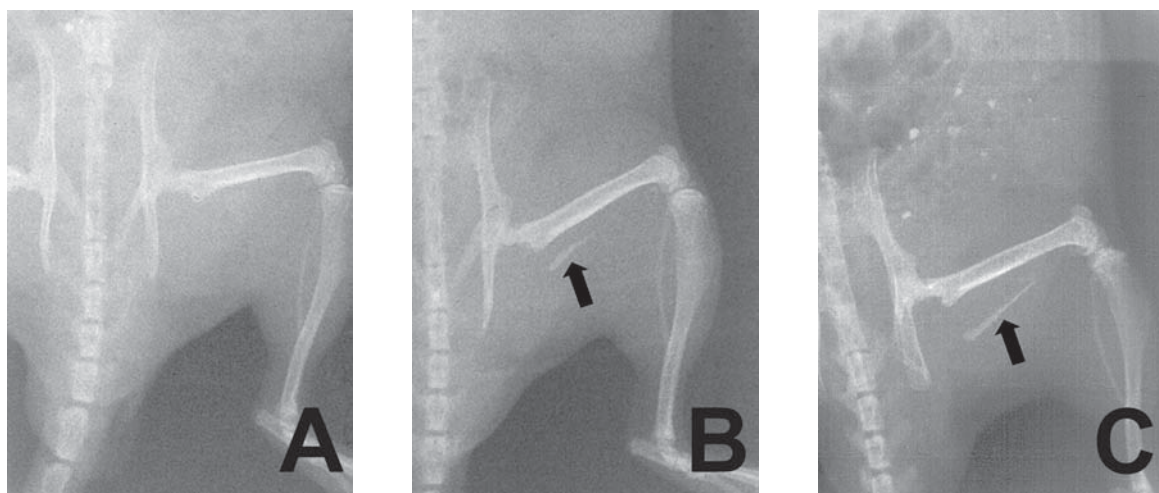


FIGURE 2 - Radiographic images of 14 days (A), 21 days (B) and 28 days (C) after implantation of matrix. Observed radiodense line (arrow) under the femur

At five and seven days post-implantation, the graft was still intact without signs of resorption on the external and internal surface or inside the old nutrient canals. The medullary canal showed traces of blood clots characterized by a fibrin network and scattered blood cells and a network of fibroblast-like mononuclear cells close to the newly formed vessels. Outside, thick, dense capsule-like

connective tissue, rich in blood vessels and fibroblast-like elongated cells arranged in layers parallel to the graft surface, was noted.

At 14 days (Figures 3A-D), the graft already showed signs of mononuclear cell-mediated resorption both on the external and internal surface, and areas of intensely basophilic cartilage tissue, mainly close to the old bone nutrient canals,

were observed. Some resorption areas inside the graft already exhibited differentiated osteoblasts and minute amounts of newly formed bone matrix. The old medullary canal was completely filled with richly cellularized and vascularized, loose connective tissue, while outside the graft the richly vascularized, capsular connective tissue became thinner.

Confirming the radiographic images, new bone formation was detected in all animals at 21 days post-implantation (Figure 4A-D). Some animals showed numerous resorption areas inside the graft, with the formation of new bone and bone marrow in these areas, while the medullary canal was found

to be resorbed and covered with loose connective tissue. In other animals, only small resorption areas were observed inside the graft, while its internal surface facing the old medullary canal was found to be resorbed and covered with newly formed bone tissue, with some bone trabeculae invading the connective tissue filling the old medullary canal which, in these cases, contained large amounts of myeloid tissue. A now thinner, fibrous external capsule was observed in all animals. A similar histological picture was observed 28 days after graft implantation, showing only an increase in the resorption areas and increased formation of new bone and myeloid tissue.

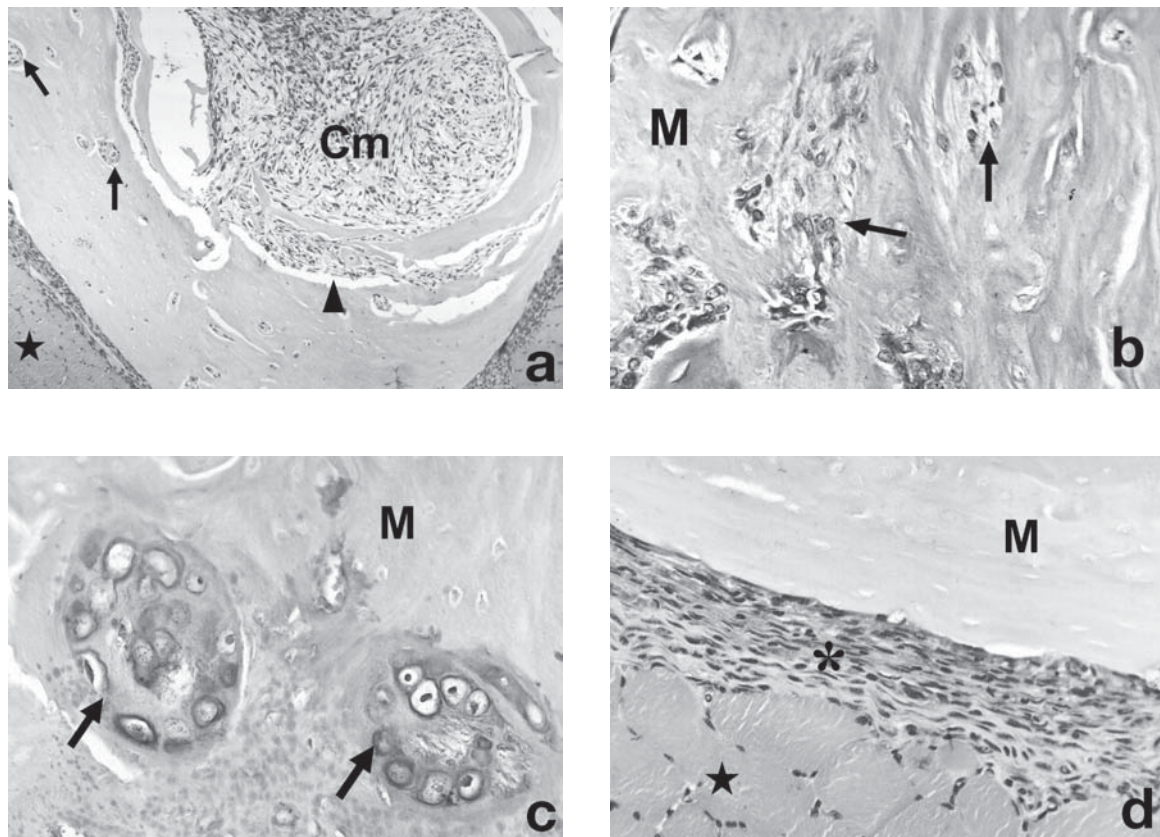


FIGURE 3 – Histologic images of 14 days: **a**) panoramic aspect of matrix (asterisk) implanted between muscle fascia (star) exhibiting spaces filled by connective tissue (arrowhead) and cartilaginous tissue (arrows). The old medullary canal (Cm) occupied by connective tissue; **b**) detail of matrix (M) showing reabsorption (arrows) by mononuclear cells; **c**) detail of neofomed cartilage tissue (arrow) inside the matrix (M); **d**) detail of the fibrous capsule between the matrix (M) and the muscle (star). Hematoxylin and eosin, magnification x34 and x340.

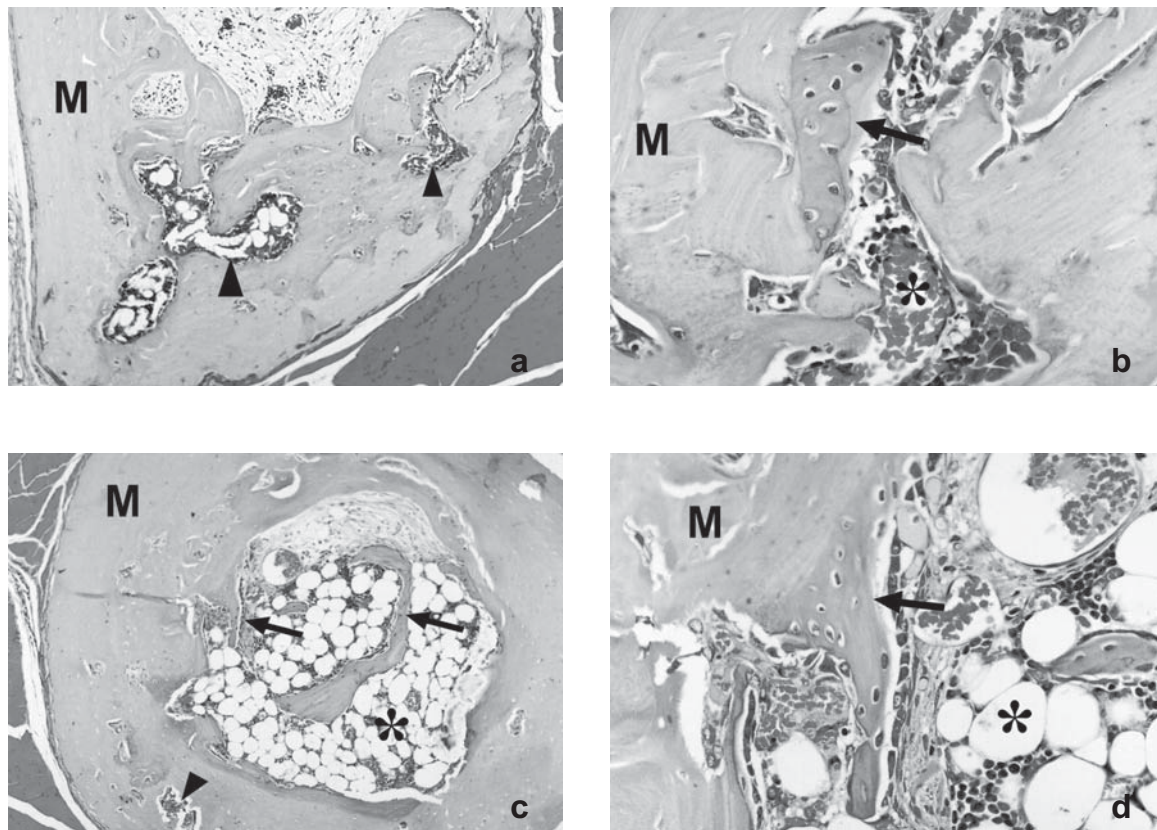


FIGURE 4 – Histologic images: 21 days; **a**) panoramic aspect of matrix (M) showing great resorption areas (arrowhead) inside the graft, with the formation of new bone and mieloid bone marrow; **b**) detail of new bone (arrows) and bone marrow (asterisc) inside the matrix (M); **c**) panoramic aspect of matrix (M) exhibiting small resorption areas (arrow) and the old medullary canal filled by neoformed bone (arrows) and bone marrow (asterisc); **d**) detail of new bone (arrow) and bone marrow (asterisc) . Hematoxilin and eosin, magnification x34 and x340.

Morphometric results

The volume density (%) of the various graft components and the number of cartilage and bone cells involved in the heterotopic osteogenesis induced in mouse muscle are shown in Figures. 5 and 6, respectively. Only 16% of the graft volume was resorbed 28 days after implantation. Resorption areas started to occur by day seven, occupying 0.4% of the graft matrix volume and increasing continuously about 12 times up to day 28 post-implantation, when they occupied 5% of the graft volume. Cartilage tissue was first detected on day 14 post-implantation in relatively large amounts, occupying 5% of the graft volume and containing 3.8×10^2 chondrocytes/mm³, the

maximum matrix and cell quantity observed throughout the experiment. The formed hyaline cartilage and the number of chondrocytes then decreased substantially, occupying only 0.3% of the graft volume and containing 0.6×10^2 chondrocytes/mm³ at the end of the 28-day observation period. Concomitantly with the presence of cartilage tissue on day 14 post-implantation, a small quantity of bone tissue was observed, occupying 0.4% of the graft volume and containing 0.2×10^2 cells (osteoblasts + osteocytes)/mm³ graft. During the subsequent periods, coinciding with the disappearance of hyaline cartilage and chondrocytes, the amount of bone tissue and the number of bone cells increased about 15 and 32 times, respective-

ly, occupying 6% of the graft volume and containing 6.4×10^2 cells/mm³ graft at the end of the 28-day study period. Myeloid tissue associated with the graft matrix (the tissue observed in the old medullary canal was not included in the quan-

tification) was first detected in small amounts on day 21 post-implantation (occupying 0.07% of the graft volume) and significantly increased up to the end of the study period (occupying 7% of the graft volume).

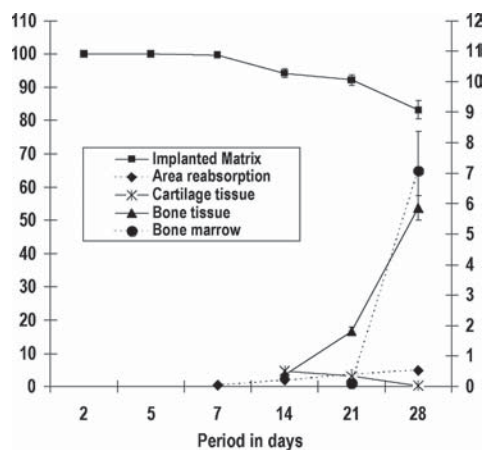


FIGURE 5 – The density volume (%) of implanted matrix, area of the reabsorption, cartilage, bone and bone marrow during the pos-implantation periods. The points are the mean \pm SEM of six mice.

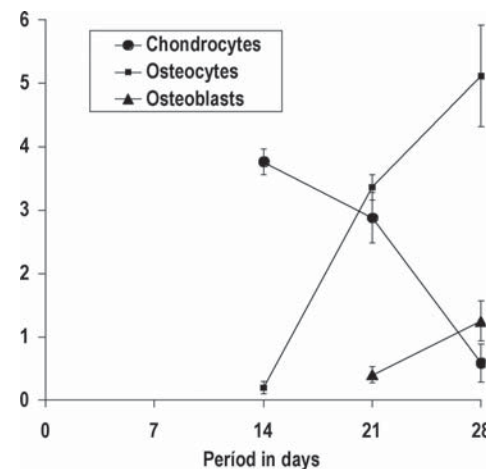


FIGURE 6 – The total number cells of the chondrocytes, osteocytes and osteoblasts during the pos-implantation periods. The points are the mean \pm SEM of six mice.

DISCUSSION

Since the 1960s it has been known that allogenic organic bone matrix is able to induce new bone formation when implanted at heterotopic sites, i.e., non-bone connective tissue such as subcutaneous tissue and perimysium, and also at orthotopic or bone sites^{6,7,11,29,30}. This inductive capacity is related to the presence of proteins, called BMPs, belonging to a group of TGF- β growth factors, inside the bone matrix which, when released into richly vascularized connective tissue, induce the morphogenetic phase of osteogenesis by endochondral ossification, i.e., a cascade of events comprising chemotaxis, migration and proliferation of undifferentiated mesenchymal cells, cytodifferentiation of chondrocytes and chondrogenesis, vascular invasion and neovascularization, cytodifferentiation of osteoblasts and new bone formation, and the occurrence of myeloid tissue^{18,29}.

The experimental model of osteoinduction at heterotopic sites, notably connective tissue associated with skeletal muscle due to its high degree of vascularization^{12,35}, has been used to determine the osteogenic potential of bone matrix as graft material and of other natural or synthetic osteoinductive materials and proteins^{2,4-5,8,13-4,22,28}, and also as a system to study osteogenesis and factors that interfere with new bone formation and regulation of bone metabolism^{15,16}. Despite its widespread use as a study and biological test model, the morphometric parameters of the events that occur during heterotopic osteogenesis in muscle connective tissue of laboratory animals such as mice, the most widely used species in tests of osteoinductive biomaterials, have not yet been established.

In the present study, initial formation of new bone tissue by endochondral ossification was demonstrated by histology in all animals of the 14-day post-implantation group, and by radiographic

and histological analysis in the subsequent groups, confirming other studies on rabbits and rats in muscle and subcutaneous sites^{3,23,27,29,36}. However, the total amount of newly formed bone tissue observed here was very small compared to these investigations. These differences might be related to the relatively young age of the animals that provided the allogenic grafts. Jergesen et al.⁸ in 1991, demonstrated that bone matrix from eight-month-old rats possessed a markedly higher inductive capacity than that obtained from one-month-old animals. Within the same context, preliminary results of studies carried out in our laboratory showed that bone proteins isolated and purified from fetal bovine bone with the molecular weight of BMPs (~18 kDa) are unable to induce heterotopic or orthotopic osteogenesis in rats.

Another possibility to explain these difference is the technique used for allogenic matrix preparation and the shape of the graft (particle or block). Preparation techniques differ in terms of the number of solvents used to remove non-collagenous proteins and in terms of the presence or absence of endogenous protease inhibitors. On the other hand, the geometry of the implant affects its osteoinductive capacity due to variations in its surface area²¹.

Cartilage tissue was also initially detected by day 14 at the highest quantity observed throughout the experiment, indicating its occurrence during an intermediate period between day seven and day 14 post-implantation. Reddi & Anderson¹⁷, 1976, in the rat, observed that chondrocyte differentiation starts by day five, followed by a marked increase in this cell population seven to eight days after implantation of the graft. It should be noted that during heterotopic osteogenesis induced by matrix BMPs the hyaline cartilage formed undergoes calcification accompanied by the death of chondrocytes and gradual disappearance of the tissue, which is replaced with newly formed bone tissue, i.e., followed by the events of embryonic and fetal endochondral ossification³.

In the present study, hyaline cartilage and chondrocytes had almost completely disappeared at the end of the 28-day study period. On the other hand, the number of bone cells (osteoblasts + osteocytes), which were first detected in a small numbers on day 14 together with a minute amount of radiographically undetectable newly formed bone matrix, showed a significant 32-fold increase 28 days after implantation, accompanied by a 15-fold increase in the quantity of newly formed bone matrix.

Another event associated with BMP-induced osteogenesis is the late formation of myeloid tissue close to the newly formed bone. Bone marrow was only detected on day 21 post-implantation, associated with areas of ossification in the graft matrix and with the old medullary canal, but had increased significantly (more than 95 times) at the end of the 28-day observation period.

CONCLUSION

The present results permit us to conclude that only a small part (16%) of the allogenic demineralized block bone matrix implanted into the connective tissue of the perimysium of the mouse thigh adductor muscle is resorbed within the first 28 days after implantation. However, during this resorption process the matrix is able to induce all events of the endochondral ossification cascade, with the formation of new bone tissue occupying 6% of the graft volume and containing 6.4×10^2 cells (osteoblasts + osteocytes)/mm³ graft.

ACKNOWLEDGMENTS

The authors are grateful to *Danielle Santi Cebolin* for technical assistance and to *Beonildes Telesinha Ruiz Correia* for typing the manuscript. The study was supported by FAPESP (Process nº 00/00877-0). Renato Yassutaka Faria Yaedú was the recipient of a scientific initiation fellowship from FAPESP (Process nº 00/05735-9). Rumio Taga is a CNPq researcher (Process nº 463077/00).

RESUMO

A osteogênese heterotópica induzida por enxerto de matriz óssea alógénica no perimílio de músculo de camundongos foi avaliada radiográfica, morfológica e morfometricamente. Diáfises de fêmures de 18 camundongos com cinquenta dias de idade, foram desmineralizados em HCl 0,6M e implantadas no músculo adutor da coxa direita de 36 camundongos. Decorreram 2, 5, 7, 14, 21 e 28 dias após-implantação, grupos de 6 animais/periódico,

foram sacrificados e radiografados, e as peças coletadas e processadas histologicamente. A análise radiográfica detectou presença de material mineralizado no enxerto somente a partir do 21º dia. Análise morfológica e morfométrica dos cortes histológicos mostrou que: a) a matriz manteve-se intacta até o 7º dia, sendo à partir dessa data reabsorvida por células mononucleadas semelhante a fibroblastos num percentual de 16% até o 28º dia; b) o tecido cartilaginoso estava presente inicialmente no 14º dia, já numa quantidade a mais alta de todo período experimental, ocupando 5% do volume do enxerto e exibindo 4×10^2 condrócitos/mm³ do enxerto. Nos períodos subsequentes a sua quantidade cresceu substancialmente, chegando ao 28º dia, com densidade de volume de 0,5% e $0,6 \times 10^2$ condrócitos/mm³; c) células e matriz ósseas foram detectadas em diminuta quantidade à partir do 14º dia, com uma densidade de volume de 0,4% e $0,2 \times 10^2$ células/mm³, aumentando ao redor de 15x e 32x, respectivamente, ao final de 28 dias, passando a ocupar 6% do volume do enxerto e a exibir 6×10^2 células/mm³. Concluímos que apesar do percentual relativamente baixo de reabsorção da matriz enxertada (total de 16%), este foi capaz de induzir todos os eventos em cascata da osteogênese por ossificação endocondral, i.e., formação e posterior desaparecimento de cartilagem hialina, diferenciação de osteoblastos e a neoformação óssea, e formação mais tardia de medula óssea hematógena.

UNITERMS

Transplante ósseo; transplante homólogo; osso; enxerto alógénico; osteogênese, ectóptica; osso, análise morfométrica; camundongo.

REFERENCES

1. Aherne W, Dunnill MS *Morphometry*. London: Edward Arnold; 1982.
2. Bessho K, Tagawa T, Murata M. Comparison of bone matrix-derived bone morphogenetic proteins from various animals. *J Oral Maxillofac Surg* 1992; 50(5):496-501.
3. Carrington JL, Reddi AH. Parallels between development of embryonic and matrix-induced endochondral bone. *Bioessays* 1991; 13(8):403-8.
4. Edwards JT, Diegmann MH, Scarborough NL. Osteoinduction of human demineralized bone: characterization in a rat model. *Clin Orthop* 1998; 357:219-28.
5. Garraway R, Young WG, Daley T, Harbrow D, Bartold PM. An assessment of the osteoinductive potential of commercial demineralized freeze-dried bone in the murine thigh muscle implantation model. *J Periodontol* 1998; 69(12):1325-36.
6. Glowacki J, Kaban LB, Murray JE, Folkman J, Mulliken JB. Application of the biological principle of induced osteogenesis for craniofacial defects. *Lancet* 1981; 1(8227):959-62.
7. Glowacki J, Mulliken JB. Demineralized bone implants. *Clin Plast Surg*. 1985; 12(2):233-41.
8. Jergesen HE, Chua J, Kao RT, Kaban LB. Age effects on bone induction by demineralized bone powder. *Clin Orthop* 1991; 268:253-9.
9. Jortikka L, Marttinen A, Lindholm TS. Partially purified reindeer (*Rangifer tarandus*) bone morphogenetic protein has a high bone-forming activity compared with some other artiodactyls. *Clin Orthop* 1993; 297:33-7.
10. Mulliken JB, Glowacki J, Kaban LB, Folkman J, Murray JE. Use of demineralized allogeneic bone implants for the correction of maxillofacial deformities. *Ann Surg* 1981; 194(3):366-72.
11. Mulliken JB, Kaban LB, Glowacki J. Induced osteogenesis—the biological principle and clinical applications. *J Surg Res* 1984; 37(6):487-96.
12. Okubo Y, Bessho K, Fujimura K, Konishi Y, Kusumoto K, Ogawa Y, et al. Osteoinduction by recombinant human bone morphogenetic protein-2 at intramuscular, intermuscular, subcutaneous and intrafatty sites. *Int J Oral Maxillofac Surg*. 2000; 29(1):62-6.
13. Pinholt EM, Solheim E. Effect of storage on osteoinductive properties of demineralized bone in rats. *Ann Plast Surg* 1994; 33(5):531-5.
14. Pinholt EM, Solheim E. Osteoinductive potential of demineralized rat bone increases with increasing donor age from birth to adulthood. *J Craniofac Surg* 1998; 9(2):142-6.
15. Reddi AH. Role of morphogenetic proteins in skeletal tissue engineering and regeneration. *Nat Biotechnol* 1998; 16(3):247-52.
16. Reddi AH. Morphogenesis and tissue engineering of bone and cartilage: inductive signals, stem cells, and biomimetic biomaterials. *Tissue Eng* 2000; 6(4):351-9.
17. Reddi AH, Anderson WA. Collagenous bone matrix-induced endochondral ossification hemopoiesis. *J Cell Biol* 1976; 69(3):557-72.
18. Reddi AH, Cunningham NS. Initiation and promotion of bone differentiation by bone morphogenetic proteins. *J Bone Miner Res* 1993; 8 Suppl 2:S499-502.
19. Reddi AH, Huggins C. Biochemical sequences in the transformation of normal fibroblasts in adolescent rats. *Proc Natl Acad Sci U S A* 1972; 69(6):1601-5.
20. Sampath TK, Muthukumaran N, Reddi AH. Isolation of osteogenin, an extracellular matrix-associated, bone-inductive protein, by heparin affinity chromatography. *Proc Natl Acad Sci U S A* 1987; 84(20):7109-13.
21. Sampath TK, Reddi AH. Importance of geometry of the extracellular matrix in endochondral bone differentiation. *J Cell Biol* 1984; 98(6):2192-7.
22. Sun L, Hu Y, Ning Z, Liang Z. The correlation between immune rejection and osteoinduction of allogeneic bone grafting. *Chin Med J (Engl)* 1998; 111(9):818-22.
23. Urist MR. Bone: formation by autoinduction. *Science* 1965; 150(698):893-9.
24. Urist MR, Huo YK, Brownell AG, Hohl WM, Buyske J, Lietze A et al. Purification of bovine bone morphogenetic protein by hydroxyapatite chromatography. *Proc Natl Acad Sci U S A* 1984; 81(2):371-5.
25. Urist MR, Iwata H. Preservation and biodegradation of the morphogenetic property of bone matrix. *J Theor Biol* 1973; 38(1):155-67.
26. Urist MR, Mikulski A, Boyd SD. A chemosterilized antigen-extracted autodigested alloimplant for bone banks. *Arch Surg* 1975; 110(4):416-28.

27. Vandersteenhen JJ, Spector M. Histological investigation of bone induction by demineralized allogeneic bone matrix: a natural biomaterial for osseous reconstruction. *J Biomed Mater Res* 1983; 17(6):1003-14.
28. Volek-Smith H, Urist MR. Recombinant human bone morphogenetic protein (rhBMP) induced heterotopic bone development in vivo and in vitro. *Proc Soc Exp Biol Med* 1996; 211(3):265-72.
29. Wang J, Glimcher MJ. Characterization of matrix-induced osteogenesis in rat calvarial bone defects: I. Differences in the cellular response to demineralized bone matrix implanted in calvarial defects and in subcutaneous sites. *Calcif Tissue Int* 1999; 65(2):156-65.
30. Wang J, Glimcher MJ. Characterization of matrix-induced osteogenesis in rat calvarial bone defects: II. Origins of bone-forming cells. *Calcif Tissue Int* 1999; 65(6):486-93.
31. Wang EA, Rosen V, D'Alessandro JS, Bauduy M, Cordes P, Harada T et al. Recombinant human bone morphogenetic protein induces bone formation. *Proc Natl Acad Sci U S A* 1990; 87(6):2220-4.
32. Weibel ER. Stereological principles of morphometry in electron microscopic cytology. *Int Rev Cytol*. 1969; 26: 235-302.
33. Wozney JM, Rosen V, Celeste AJ, Mitsock LM, Whitters MJ, Kriz RW, Hewick RM, Wang EA. Novel regulators of bone formation: molecular clones and activities. *Science* 1988; 242(4885):1528-34.
34. Wu ZY, Hu XB. Separation and purification of porcine bone morphogenetic protein. *Clin Orthop* 1988; (230):229-36.
35. Yoshida K, Bessho K, Fujimura K, Kusumoto K, Ogawa Y, Tani Y et al. Osteoinduction capability of recombinant human bone morphogenetic protein-2 in intramuscular and subcutaneous sites: an experimental study. *J Craniomaxillofac Surg* 1998; 26(2):112-5.
36. Yu YM, Becvar R, Yamada Y, Reddi AH. Changes in the gene expression of collagens, fibronectin, integrin and proteoglycans during matrix-induced bone morphogenesis. *Biochem Biophys Res Commun* 1991; 177(1):427-32.
37. Zhu B, Pu Q, Chen N, Chen S. Expression, purification, and bone-inducing activity of recombinant human bone morphogenetic protein-3 mature peptide. *Chin J Biotechnol* 1999;15(3):153-8.

Recebido em:30/10/03

Aprovado em:03/11/03

Rumio Taga

Departamento de Ciências Biológicas – Histologia

Faculdade de Odontologia de Bauru – USP

Al. Octávio Pinheiro Brisolla, 9-75Z

zip Code: 17012-901

Bauru – SP, Brazil

Tel: (14) 2358259

cestari@fob.usp.br